



## Dynamic studies on the inhibitive action of magnesium stearate on hot corrosion in a kerosene fired Furnace

**Mahmood M. Barbooti\***, **Safa A. Al-Niaimi**, **Kadhun F. Al-Sultani**,

*Department of Chemical Engineering, University of Technology, Baghdad, Iraq.*

Received 2012, Revised 28 March 2012, Accepted 28 March 2012.

\*Corresponding Author: Email: [brbt2m@gmail.com](mailto:brbt2m@gmail.com),

Present address: Earth and Environmental Studies Department, Montclair State University, Normal Ave 1, Montclair, New Jersey 07043, USA.

### Abstract

The inhibitive effect of magnesium stearate (MS) on the hot corrosion of steel structures of power generation station was studied using a kerosene fired furnace. Three steel alloys were selected including [SA 178A, 209 T1, 213 T11, ASME Code], prepared as rectangular pieces (10 x 20 x 5 mm) from water wall tubes and superheater tubes of a local power station. The specimens were mechanically polished with emery paper (100, 320, 600 and 1000) under running tap water and rinsed with distilled water and benzene. The heating chamber of the furnace had shelves on which specimens are placed. The vanadic slag (synthetic ash) chosen was an intimate mixture of 67% wt ( $V_2O_5$ ) and 33% wt ( $Na_2SO_4$ ). Mixtures of magnesium stearate, MS: synthetic ash of 1:1, 1:2 and 1:3 molar ratios of were applied onto the surface of the specimens. The heating program was carried out at various time intervals (2-10 h) to study the normal oxidation at different temperature (550-950°C). Constant time heating programs involved heating at the specified temperatures for 4 h. The rate of oxidation is accelerated in the presence of vanadic slag (mixture of  $Na_2SO_4$  with various Na-V-O bronzes and resulted in increased corrosion rate with increasing temperature (550-950° C). X-ray diffraction analysis indicated the presence of iron oxide ( $Fe_2O_3$ ) with the vanadic slag materials. The weight loss of the three alloys specimens indicated a Clear reduction in the degree of corrosion with increasing MS content. The scale changed into a powder form that can be easily removed from the surface of the specimens. The best ratio from MS: Ash is 3:1, which gave inhibition efficiency of 85% at 550°C. The inhibition efficiency increases with temperature decrease. With the introduction of MS with the ash magnesium vanadate  $Mg_3V_2O_8$  was a major constituent together with some MgO resulting from the thermal decomposition of MS.

**Key Words:** *Hot ash corrosion, Magnesium Stearate, Steel structures, corrosion inhibition, Power generation stations*

### Introduction

Ash fouling and flame-side corrosion of metal surface, together with heat transfer surface fouling are major problems in power generation stations when burning heavy oils. Vanadium occurs in the form of porphyrinic and non-porphyrinic in crude oils [1]. These compounds decompose in the gas stream to give mainly vanadium pentoxide ( $V_2O_5$ ), which is most damaging due to its low melting point (690°C) i.e. it is in its liquid state at normal combustion temperature. Sodium in the oil is mainly present as (NaCl) and is readily vaporized during the combustion process [2]. The presence of a liquid phase on the surface of a metal is usually necessary for corrosion reactions to occur at high rates. The most likely liquid phases are based on vanadium pentoxide and sodium sulphate complexes depending upon the exact analysis of the fuel used [3]. A series of compounds are formed between ( $Na_2O$ ) and ( $V_2O_5$ ), some of which have melting points below the operating temperature of boilers and turbines. The eutectic formed between ( $5Na_2O.V_2O_4.11V_2O_5$ ) and

sodium meta-vanadate ( $\text{Na}_2\text{O} \cdot \text{V}_2\text{O}_5$ ) melts at ( $527^\circ\text{C}$ ). However, under an atmosphere containing oxides of sulphur, other components can form e.g.  $\text{Na}_2\text{SO}_4$ ,  $\text{Na}_2\text{S}_2\text{O}_7$ ,  $\text{V}_2\text{O}_5 \cdot 2\text{SO}_3$  and  $\text{V}_2\text{O}_5 \cdot \frac{1}{2} \text{SO}_3$  [4].

Prevention of hot corrosion is impossible and a reduction can be effectively performed. In contaminated combustion atmospheres, there are three basic ways to reduce the hot ash corrosion problems and these are:-

- I-Removal of harmful impurities presents in the environment.
- II-Addition of a compound to counteract the harmful impurities .
- III-Changing the combustion condition (fuel treatment and control of burning) to minimize attack.

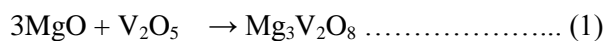
Combustion Control can be done to minimize corrosion problems in boilers and turbines. The use of water-in-oil emulsions (in which each fuel droplet leaving the atomizer contains a number of micro-droplets of water) is a promising technique to reduce smoke and ( $\text{NO}_x$ ) emissions from boilers and gas turbines. Other possible benefits include the reduction in excess air with consequent reduction in  $\text{SO}_3$  formation and the elimination of metal-containing antismoke additives and the resulting deposits and fouling in gas turbines, the ability to use heavier and cheaper fuel [5].

The use of corrosion resistance coatings for existing alloys has found widest application in the gas turbine and boiler field. Metallic coating has been applied by electrodeposition, high temperature diffusion coating and plasma spraying [6]. The effect of ceramic coatings has also been investigated. The metallic coatings examined were principally those of silicon, chromium, aluminum, zirconium and beryllium [6]. The higher the chromium content of the alloy, the better would be the hot-corrosion resistance [7]. El-Dahshan [8] observed that Co-Cr-W alloys were more resistant to oxidation than (Ni-Cr-W) alloys when coated with sodium sulfate.

Gagliano et al., [9], found that high-chromium (low molybdenum) weld overlay and FeCr and SiCr coating materials may provide enhanced corrosion resistance for superheater/reheater tubing operating under advanced ultra-supercritical conditions [ $760^\circ\text{C}$  ( $1400^\circ\text{F}$ ) steam temperature and pressures in excess of 35 MPa (5000 psi)]. Mifune et al, [10] studied the behavior of thermal barrier coatings by comparing double-layer coatings and graded coatings against  $\text{V}_2\text{O}_5$ - $\text{Na}_2\text{SO}_4$  corrosive ash. They applied two types of oxide ceramics with a bond coating of NiCrAlY, to metallic substrates. Thermally sprayed coatings on boiler tubes were mainly attached through oxides and voids at splat boundaries. They presented a promising method for producing homogenous coatings [11].

The corrosive effect of ash-causing contaminants, principally vanadium, can be neutralized by chemical additives. The additives work by forming a stable vanadate of higher melting point than the vanadium compounds originally present, thus preventing formation of a liquid phase at the operating temperature [12].

Magnesium compounds additions, however, raise the melting point of the deposit appreciably from  $680^\circ\text{C}$  for  $\frac{1}{2}\text{MgO} \cdot \text{V}_2\text{O}_5$  to  $1100^\circ\text{C}$  for  $3\text{MgO} \cdot \text{V}_2\text{O}_5$  and have been found to be very effective [13]:



The  $\text{Mg}_3\text{V}_2\text{O}_8$  is solid at the operating temperature of industrial boiler tubes and turbine blades [14]. When sufficient  $\text{SO}_3$  is present, MgO can be sulphated to  $\text{MgSO}_4$ , which can then react with  $\text{V}_2\text{O}_5$  to form magnesium pyrovanadate which may be molten on the surface boiler tuber and turbine blades [13]:



Thus, corrosion control in low grade or residual fuel oils is modified by the presence of ( $\text{SO}_3$ ) [15]. Blauenstein [16] injected dispersed magnesia additive with the fuel and could gain benefits on a 300 MW oil-fired boiler such as improved combustion, reduction in total particulate emissions and reduction in metallic corrosion as indicated by higher pH ash and confirmed by iron determinations on the ash. An ideal additive should be miscible with fuel oil and improve combustion conditions, especially atomization.

Barbooti et al. studied the inhibitive action of magnesium oxide and magnesium sulphate [17] on the hot ash corrosion by heating alloy specimens from the hangers on which tubes are suspended, in an electrical furnace and following the inhibition by weight loss an chemical analysis of the scale. Nishikawa et al [18] have studied the effect of Mg-Additive against high temperature fouling and corrosion. When Mg was added, weight loss due to high temperature corrosion was reduced to about equal level of corrosion by clean kerosene firing in the temperature range below 700°C. Timokhin et al, investigated the corrosion inhibitive action of magnesium stearate, MS [19].

The present work is a dynamic study of the action of magnesium stearate, MS, as an inhibitor of hot ash corrosion using pilot scale kerosene fired furnace.

## EXPERIMENTAL

### Materials and Chemicals

The test specimens were prepared from three of the alloys used in boilers (water wall tubes and superheater tubes) including SA 178A, 209 T1 and 213 T11. Boiler tubes pieces were supplied from South-Baghdad Power generation Station. The chemical composition and mechanical properties of the alloy used in this work is shown in Tables 1 and 2, respectively [20]. Magnesium stearate was a pharmaceutical grade material supplied by a Ibnul-Beetar State factory of pharmaceutical materials with a purity of 98.5%.

**Table 1:** chemical composition of steel alloys [18]

Component	SA -178	209 T1	213 T11
C	0.06-0.18	0.1-0.2	0.08-0.15
Mn	0.27-0.73	0.3-0.8	0.3-0.6
P (max).	0.035	0.025	0.025
S (max)	0.035	0.025	0.025
Fe	Remain	Remain	Remain
Si	0.1-0.5		0.5-1
Mo	0.044-0.65		0.44-0.65
Cr		1-1.5	

**Table 2:** mechanical properties of steel alloys [18]

Property	SA -178	209 T1	213 T11
Resistance (Mpa)	325 min	380	585
Tensile strength (Ksi)	47	55	85
Limit elastic (Kpa)	180	205	415
Yield strength(Ksi)	26	30	60
Allong. elong. (%)	30	30	20

A kerosene fired furnace was designed and installed specially for this study. The details and calculations involved in the design and performance of the furnace were discussed elsewhere [21].

### Procedures

The test specimens were cut from these pipes into rectangular pieces (10 x 20 x 5 mm) (w x l x t). The specimens were mechanically ground with emery paper (100, 320, 600 and 1000) under running tap water

and rinsed with distilled water, benzene, then these specimens were dried and left in a vacuum desiccators and weighed with a semi-micro balance.

The vanadic slag (synthetic ash) chosen for this work was based on 67% wt ( $V_2O_5$ ) and 33% wt ( $Na_2SO_4$ ). This mixture was chosen because it has been shown to be the most representative corrosive simulated by other workers [17, 22]. The calculated amounts of  $V_2O_5$  and  $Na_2SO_4$  in the ratio molar ratio of 3:1 were weighed and ground in an agate mortar for 15 minutes. The slag mixture was then stored in desiccators until required for use.

The calculated amounts of magnesium stearate, MS, were mixed with and 10 g synthetic ash with 3 mls of acetone. With the aid of a syringe the mixture was applied onto the surface of the cleaned specimens. Three molar ratio mixtures were prepared (MS: ash): 1:1, 2:1 and 3:1. The tests were carried out at various time intervals (2, 4, 6, 8 and 10 h) to study the normal oxidation at different temperature (550, 650, 750, 850 and 950 °C). Constant time tests involved heating at the specified temperatures for 4 h. At the end of the run, the furnace is switched off and samples are taken out after 24 h. The specimens are dipped in caustic soda solution containing zinc dust (20% NaOH + 200g Zn/L.), at 60°C for five minutes, and abraded with emery paper grades (100, 320, 600 and 1000) respectively under running tap water, then rinsed with water and kept over silica gel for one hour, and finally weighed to the fourth decimal.

## Analysis

The exposed specimens were examined for the color and appearance of corrosion products and the extent of spallation, using a Cambridge scanning electron microscope (England) model 240-12. X-ray diffraction measurements were carried out on a Phillips X-ray Diffractometer, Type PW1050 Holland with iron target to produce an x-ray beam of wavelength of Fe- $\alpha$  at 1.93 Å. The measurement conditions were: tube current of 20 mA, a voltage of 40KV and a scan speed of  $2^\circ(2\Theta)/1\text{cm}$  were used. Reference was made to the ASTM card Index.

## Results and Discussion

### Effect of Vanadic Slag:

Fig. 1 shows the weight loss of the steel specimens after 4 h exposures time to temperatures of 550 – 950° C as affected by the coating with the vanadic slag. When these results were compared with those for the uncoated specimens, it appeared that the increase in heating time, leads to an increase in weight gain. Numerically, at 850° C, the amounts of weight gain for (SA-178A) and 213 T1 specimens in the presence of the synthetic ash were 0.16 and 0.14 kg/m<sup>2</sup>, respectively. This is compared with only 0.013 and 0.011 kg/m<sup>2</sup> for the weight gain values of the uncoated specimens.

The vanadic slag highly accelerated oxidation/hot corrosion of the alloys and most of the weight gain occurred within the high temperature regions (750, 850 and 950 °C). Above 650 °C, many sodium-vanadium bronzes such as  $NaVO_3$ ,  $Na_2O.V_2O_5$ ,  $Na_2O.3V_2O_5$ ,  $Na_2O.6V_2O_5$  and  $Na_2O.V_2O_4.5V_2O_5$ , are formed [20]. These compounds catastrophically oxidize the alloy components acting as oxygen carriers, metal oxide distorts, or dissolving agents of the protective oxide layer [20]. The scale formed after the thermal treatment is sticky and metallic in color.

The X-ray diffraction investigation indicated the formation of sodium vanadate (Fig. 2). This is the most important aggressive species in the (Na-V-O) system which became appreciable after the melting of the eutectic mixture ( $Na_2SO_4 - V_2O_5$ ) and increase with temperature. Therefore ( $Na_2SO_4$ ), which has no individual aggressive behavior towards the metal, facilitates the low temperature melting of the ash and initiates the formation of sodium vanadate, which attacks the metal surfaces [23].

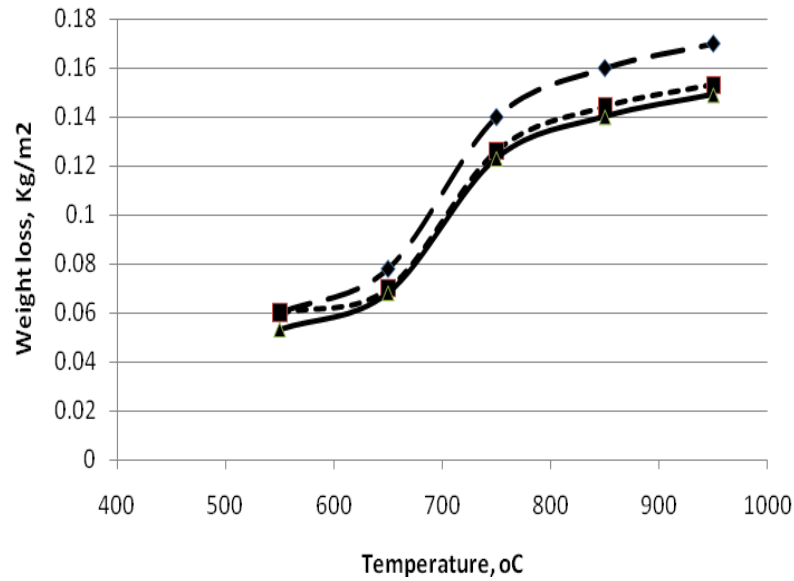


**Figure 1:** Weight loss after 4 h exposure at 950°C for  $\blacklozenge$  SA 178;  $\blacksquare$  209 and  $\blacktriangle$  213 steel specimens coated with vanadic slag.

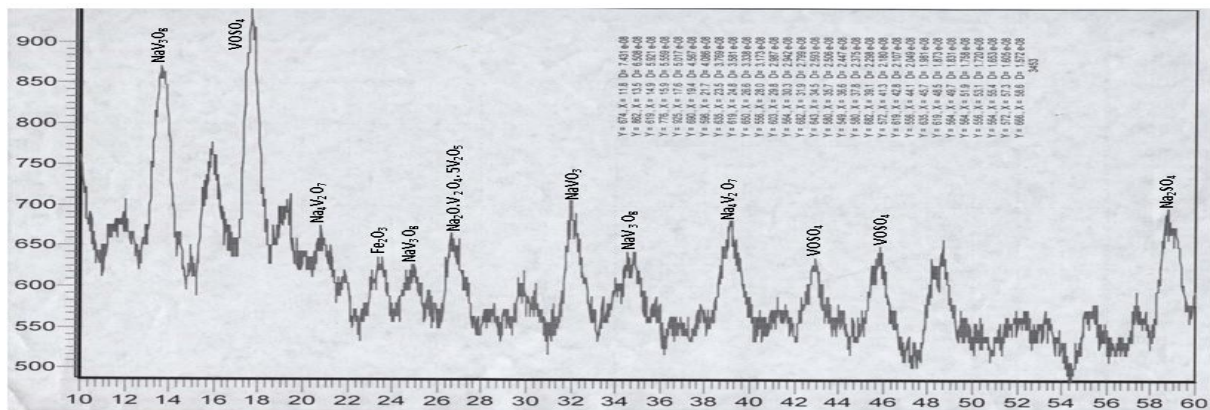


**Figure 2:** X-ray Diffractogram of Deposits for (SA-178) Specimen Coated with Ash after Heating at 750°C for 4h.

For the 209 T1 alloy the effect of ash on the steel surface confirmed the oxidation of iron and its dissolution of  $\text{Fe}_2\text{O}_3$  in the molten scale in addition to the formation of several types of sodium vanadates. The sodium-vanadium bronzes, namely:  $\text{NaV}_3\text{O}_8$  (6.508, 3.58 and 2.593 Å),  $\text{Na}_2\text{O.V}_2\text{O}_4.5\text{V}_2\text{O}_5$  (3.338 Å),  $\text{Na}_4\text{V}_2\text{O}_7$  (4.08 and 2.298 Å). The thermal treatment also resulted in the formation of vanadyl sulfate ( $\text{VOSO}_4$  and its main peaks (5.017, 2.107 and 1.981 Å) predominate at the diffraction pattern. Similarly residual sodium sulfate could be identified,  $\text{Na}_2\text{SO}_4$  (1.572 Å) and iron oxide ( $\text{Fe}_2\text{O}_3$ ) at 3.769 Å.

### Effect of Magnesium Stearate Addition:

Figs. 3-5 show the weight losses of the three specimens coated with mixtures containing increasing amounts of MS with constant amount of the vanadic slag at the molar ratios of MS: slag of 1:1, 2:1 and 3:1. The results indicated reduction in weight losses with increasing MS content. The mole ratio 3:1 was very effective against high temperature corrosion due to the ash slag. However the deposits were physically weak so that they are easily removed by simple tapping of the specimen [24].

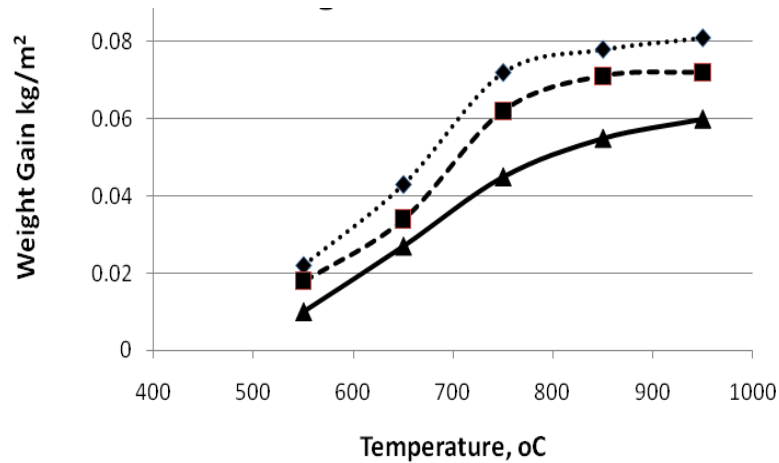


**Figure 3:** Action of Magnesium Stearate Addition on Weight Gain for (213 T1) Specimens at 1:1, dotted line; 2:1, dashed line and 3:1, solid.

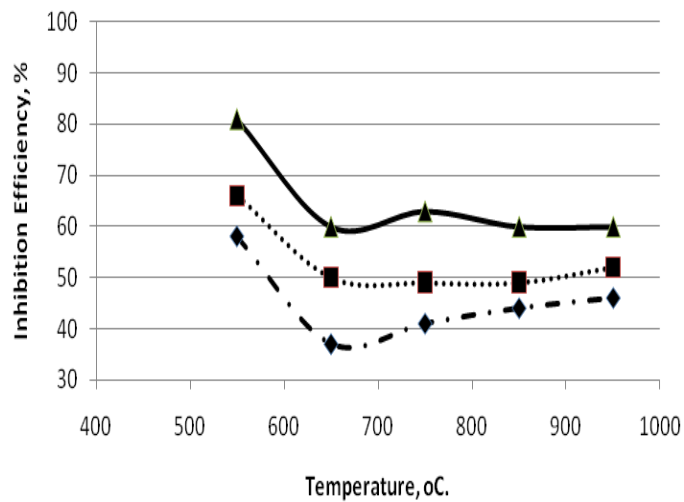


**Figure 4:** Inhibition efficiency of  $MgC_{36}H_{70}O_4$  at 1:1,  $\diamond$ ; 2:1,  $\blacksquare$  and 3:1,  $\blacktriangle$  mole ratios of MS:V Slag for (SA-178 A) Specimens for 4 h exposure.

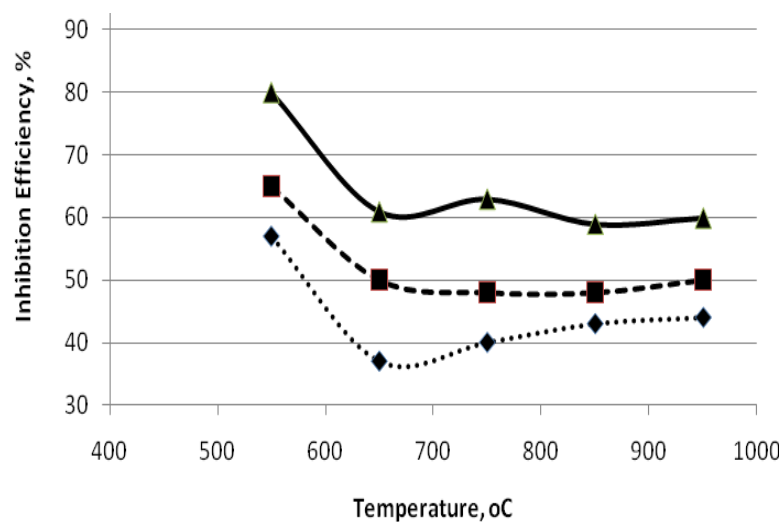


**Figure 5:** Corrosion Inhibition Efficiency of Mg Stearate, for (213 T11) Specimens at (4h)

These results proved that the MS was sufficiently effective against high temperature corrosion in the temperature range where the boiler-superheated tube was commonly used. It is clear that the inhibition

efficiency increases with the increase of the mole ratio of additive and ash. The optimum additive to ash ratio is 3:1, which gave inhibition efficiency of 80% at (550°C).

The inhibition Efficiency was calculated according to eq. 3.

$$\text{Eff}_{\text{Inh}} \% = [(w_0 - w_i) / w_0] \times 100 \dots\dots\dots (3)$$

Where  $w_0$  is the weight loss in the presence of [ash] and  $w_i$  is the weight loss in the presence of [ash + MS].

The inhibition efficiencies of MS addition together with the numerical evaluation of weight loss values of the three specimens are given in Tables 3-5. Additives containing magnesium (Mg) are used primarily to control vanadic oxidation deposition and function by modifying ash composition and increasing ash melting point. Through combustion ( $V_2O_5$ ) at an appropriate (Mg/V) treatment ratio, magnesium orthovanadate ( $3MgO \cdot V_2O_5$ ) with melting point of about (1243°C) is formed as a new ash component [25], however the addition may increase the deposits, and at the same time deposits are physically weak so that they are easily removed by simple tapping of the specimens [24].

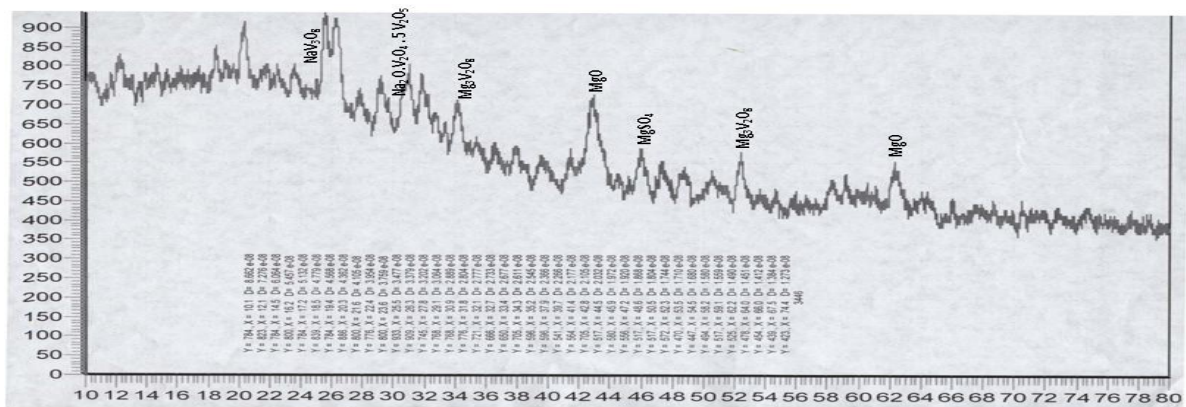


Figure 6: X-ray Diffractogram of Deposits for SA-178A Specimen Coated with [1:1] MS:Ash after Heating at 750° C for 4h

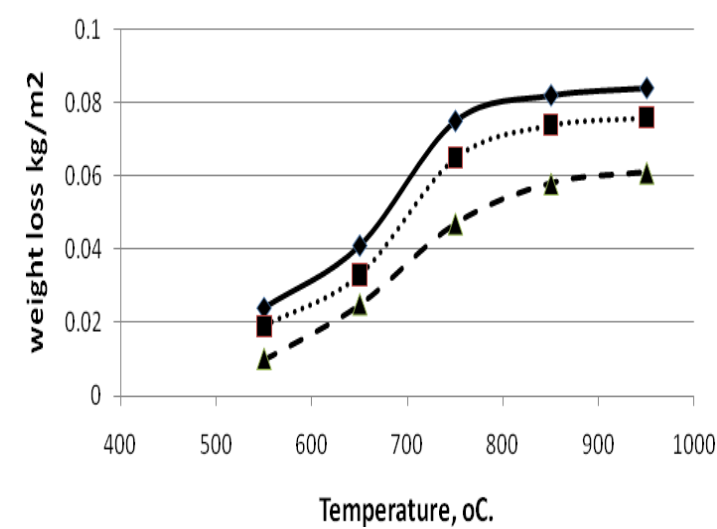


Figure 7: Action of Magnesium Stearate Addition on Weight Gain for (209 T1) Specimens at 1:1, solid line; 2:1, dotted line and 3:1, dashed line.

For (SA-178A) alloy, the constituents of the coating or the scales of the corroded specimens were identified by X-ray diffraction analysis. Fig. 6 shows the diffraction pattern of the scale resulted from the synthetic ash after heating at (750°C) for (4h). level of the natural oxidation.

The main peaks of sodium vanadates  $\text{NaVO}_3$  [2.799 Å] and  $\alpha\text{-NaVO}_3$  [2.097 Å] could be identified together with ferric oxide at 3.66 Å. This is an indication of the role of molten sodium vanadate on introducing oxygen to react with the iron surface so that it catalyzed the oxidation of the metal. Furthermore, the insitue formed oxide dissolves in the molten layer of the ash compounds and causes the gradual depletion of iron.

The inhibition Efficiency was calculated according to eq. 3. Fig. 7 shows the action of MS addition on the weight loss of steel 209 T1. It is clear that MS inhibited the corrosive action of vanadium slag such that the loss at the highest temperature range the loss could be reduced to the

### Metallographic Examination (SEM)

The scanning electron microscopy (SEM) was of valuable assistance in providing more information about the surface morphologies [26]. Fig. 8 shows typical feature of the corroded alloy (SA-178A) after exposure to ash (67 wt.%  $\text{V}_2\text{O}_5$ : 33wt.%  $\text{Na}_2\text{SO}_4$ ) at (850°C) for (4h). Many voids can be seen in places running together forming porosity within the underlying surface beneath the slag-containing, oxide layer ( $\alpha\text{-Fe}_2\text{O}_3$ ). Thus, vanadium pentoxide-sodium sulfate induces severe corrosion of the alloy AS-178A.

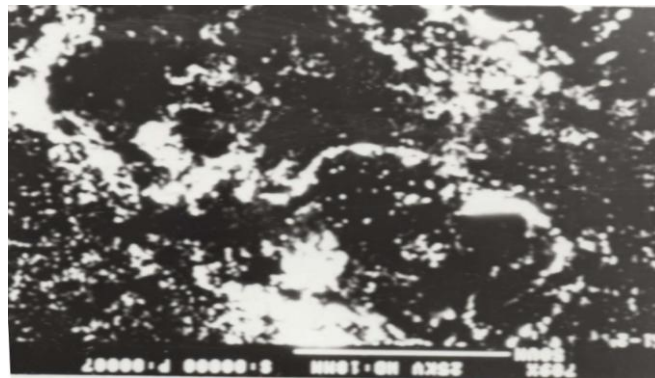


**Figure 8:** SEM Micrographs of (AS-178A), Specimen Corroded in Ash (67Wt. %  $\text{V}_2\text{O}_5$ :33 Wt.%  $\text{Na}_2\text{SO}_4$ ) at (850°C) and time (4h) using 500 times magnification..

The SEM photomicrograph, of the 209T1 alloy after exposure to ash at (850°C) for (4h), indicated deep secondary cracks and a few facets that suggest quasi cleavage [27]. These images showed that the attack by ash proceeds in a uniform manner sometimes and in a more localized and intensive fashion at other time. It is initiated at the scale metal interface and is gradually propagated downwards, followed by lateral drenching as the cracks interconnect [28].

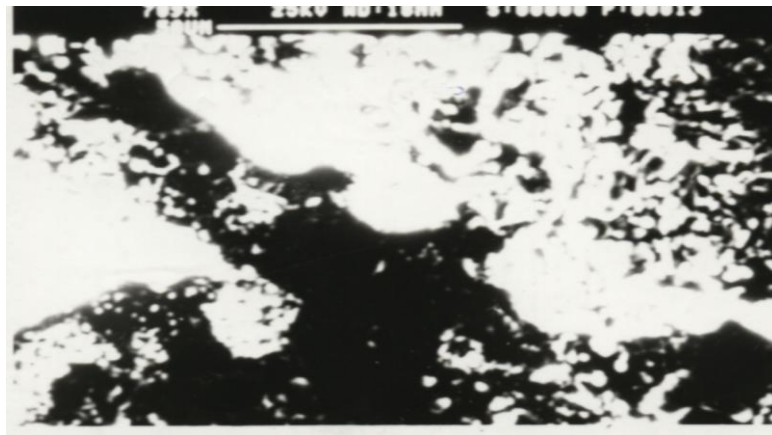
For the 213 T11 Alloy there appeared dimpled rupture clearly secondary cracks with string type characteristics probably reflecting the orientation of the original rolling direction [27]. Local damage was observed after [850 °C and 4 h] of exposure and products when analyzed SEM/X-ray diffraction techniques revealed oxides of the base metal elements. The increase chromium – containing alloy showed better resistance of hot corrosion.

Fig. 9 shows the SEM of the SA-178 alloy surface coated with ash and additives at a molar ration of 1:1 at temperature of 850°C. The surface seems to be relatively weak space fatigue striations with fewer secondary crackings [25].



**Figure 9:** SEM Micrographs of Specimen SA-178A coated with 1:1 Ash:MS and heated at 850°C for 4h, using 500 times magnification.

Thus, the presence of ash with the additive at such molar ratio indicated minimal attack on alloy SA-178A and the coating is less aggressive than in the absence of the additive. Further increase of the additive to 1:3 has inferior action of the hot ash as can be seen in Fig. 10. The SEM revealed additional small dimples that are not readily apparent at the (700x) magnification [27].



**Figure 10:** SEM Micrographs of (AS-178A), Specimen Coated with Ash and Additive (1:3) at (850°C) and (4h), using 500 times magnification.

After MgO is formed from the thermal decomposition of MS and its particles deposit on the specimens, it reacts with the oxides of vanadium to form magnesium orthovanadate  $Mg_3V_2O_5$ . Other possible magnesium compounds such as  $Mg_2V_2O_7$  and  $MgV_2O_6$  were detected in the deposits by X-ray diffraction techniques [28]. In contrast, the addition of NiO leads to the formation of  $Ni_3V_2O_8$ , a refractory compound that dramatically reduces the corrosiveness of the ash materials by trapping vanadium [29].

### Microstructure Examination

The micrograph of the unfired, uncoated ( SA-178A) specimen was taken from midthickness of wall in longitudinal section is shown in Fig. 11. The microstructure was referred to some standard data [30], and indicated the existence of ferrite ( light areas ) and pearlite ( dark areas). The second examination shown in Fig.(5-45 ) refers to the coated specimen with ash only after heating at (950 °C) for ( 4h). The structure mainly consists of ferrite (white constituent) and small amount of pearlite (dark constituent) [31]. Thus, high temperature leads to dispersion pear lite with increase time [32].

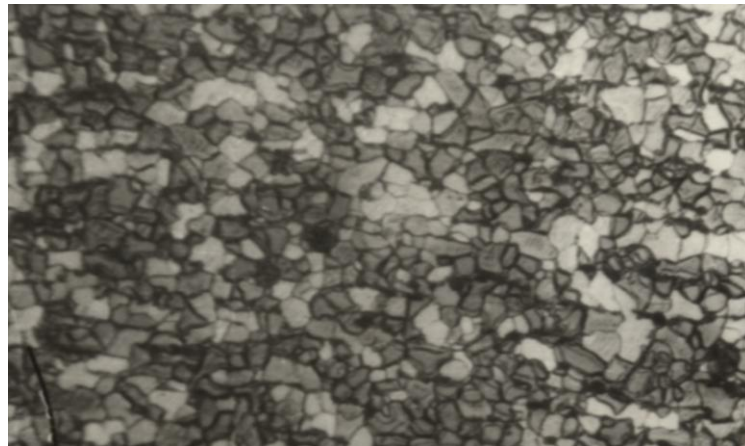


**Figure 11:** Optical Micrographs of unfired SA-178A) specimen, using 500 times magnification.

The micrograph of specimen coated with ash and additive at mole ratio 1:1 and 1:3 additive treatments at (950 °C) is shown at Figs. 12 and 13, respectively. The structure consists of ferrite and to some extent pearlite [33].

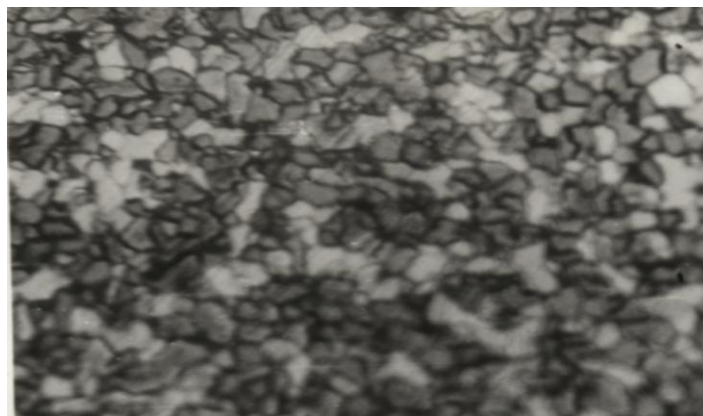


**Figure 12:** Optical Micrograph of Specimen SA-178A coated with 1:1 Ash:MS and heated at 950°C for 4h, using 500 times magnification.



**Figure 13:** Optical Micrograph of Specimen SA-178A Coated with 1:3 (Vanadic Slag: MS) and fired at 950°C for 4h, using 500 times magnification.

## Conclusion

Magnesium stearate which is the mineral salt of an Stearic acid proved good candidate as a hot corrosion inhibitor for steel structures in in power generation stations. The inhibitive action of the material was tested on steel specimens from various parts of the power plant coated with synthetic ash which is usually a combination of sodium sulfate and vanadium pentoxide. The additive was applied at various mole ratios to synthetic ash and fired in a dynamic system of kerosene fired furnace. Weight loss measurements as well as X- ray diffraction and microstructure examination were employed to follow the inhibitive action of magnesium stearate on the hot ash corrosion. In addition to the preventive activity of magnesium stearate, the residual materials on the steel specimens were in the form of easily removed form due to the formation of high melting magnesium vanadate and restoring the surface of the steel structures.

## References

1. Barbooti M.M., Said E. Z., Hassan E. B., and Abdul-Ridha S. M., "Separation and spectrophotometric investigations of the distribution on nickel and vandium in heavy crude oils", *Fuel*, 68 (1989) 84.
2. Johnson, D.M., Whittle, D.P and Stringer, J., "Corrosion Sci., "Mechanisms of Na<sub>2</sub>SO<sub>4</sub>-induced accelerated oxidation", 721 (1975) 15.
3. Williams, F. A and Crawley, C. M. "Impurities in Coal and Petroleum, The Mechanism of Corrosion by Fuel Impurities", Butterworths, London, 1963, pp 24-67.
4. Kristensen, P. G., Karll, B., Bendtsen, A.B., Glarborg, P., and Dam-Johansen, K., "Exhaust Oxidation of Unburned Hydrocarbons from Lean-Bum Natural Gas Engines *Combust. Sci. Technol.* 157 (2000) 263.
5. Zwillenberg, M.L., Sengupta, C and Guerra, C.R., "Water\ oil emulsion Combustion in Boilers and Gas Turbines", Engineering Foundation Conference, New England College, New Hampshire, July-26, 1977.
6. Alexander, K.B. , PruBner, K., Hou, P.Y. and Tortorelli, P. F. "Micro-Structure of Alumina Scale and Coating on Zr-Containing Iron Aluminide Alloys", *Microscopy of Oxidation* 3.246-255. J.B. Newcomb and J.A. Little Eds., The Institute of Metals. 1997.
7. Page, K. and Taylor, R.J. in Hart A.B. and Cutler, A.J.,(Eds.)" Deposition and Corrosion in Gas Turbine", Applied Science, London, 1973, P (350).
8. EL- Dahshan, M.E., "Study of Co-Cr-W alloys to resist oxidation in the presence of sodium sulfate", Proc. 1<sup>st</sup> Arab Conf. Corrosion, Kuwait, 1987, PP 347-361.
9. Gagliano, M. S., Hack, H. and Stanko, G., "Fireside Corrosion Resistance Of Proposed Ultra supercritical Superheater and Reheater Materials: Laboratory and Field Test Results", 33th International Technical Conference On Coal Utilization & Fuel Systems, Fl., USA, June 1 – 5, 2008.
10. Mifune, N., Harada, Y., Doi, T. and Yamasaki, R., "Hot-Corrosion Behavior Of Graded Thermal Barrier Coatings Formed By Plasma-Spraying Process", *J. Thermal Spray Technol.*, 13 (2004) 561-569.
11. Rezakhani, D., "Corrosion behaviors of several thermal spray coatings used on boiler tubes at elevated temperatures", *Anti-Corrosion Methods and Mater.*, 54 (2007) 237 – 243
12. Rapp, R.A., "Hot Corrosion of Materials", *Pure and Appl. Chem.*, 62 (1990), 113-122.
13. Rhys-Jones, J.R. , Nicholls, T.N. and Hancock, P., "Effects of SO<sub>2</sub>/SO<sub>2</sub> on the efficiency with which MgO inhibits vanadic corrosion in residual fuel fired gas turbines", *Corr. Sci.*, 23 (2) (1983) 39-44.
14. Hancock, P., "Corrosion of Alloys at High Temperature in Atmospheres Consisting of Fuel Combustion Products and Associated Impurities". H.M50, 1968.
15. Hancock, P., "The use of laboratory and rig tests to simulate gas turbine corrosion problems", *Corrosion Sci.*, 23 (1982) No.51.
16. Blauenstein, E., "Engineering found. Conf., New England College, New Hampshire, July-26, 1977.
17. Barbooti, M.M., AL-Madfai, S.H. and Nassonri, H. J., "Thermochemical studies on hot ash corrosion of stainless steel 304 and inhibition by magnesium sulphate", *Thermochim. Acta.*, 1988, 126, 34-49.

18. Timokhin, I. A., Lukashevich, I. P., Shekhter, Y. N. and Fertman, E. V., "Polar and protective properties of magnesium salts of organic acids, *Chemistry and Technology of Fuels and Oils*, 9 (2004) 144-147.
19. Nishikawa, E., Kaji, M. and Ishigai, S., *Proc. ASME, JSME Therm. Eng. Conf.*, 1983, Vol.1, , PP 545-52.
20. Francois, R. Thiorry, L. and Benoit, L. "Piping Equipment / Materials Petrole", *Trouvay and Cavrin, API, ASTM, ASME Standard*, 1998.
21. Al-Sultani, K.F., *Ph. D. Thesis, Univ Technology*, 2003.
22. Barbooti, M.M., "Inhibition of Hot ash corrosion of boiler tube steels with magnesium oxide direct addition to fuel oil., *Proc. 1<sup>st</sup> Conf. Chem. Petrochem. Ind. (Chem-Arab)*, Beirut, 2001, 10-14 Jan.
23. Malik, A.V. and Ahmed, S., , "'Oxidation behavior of silicate, chromate and oxide coated 303 steel in presence of ionic salts in Temperature 400-1000 oC", *British Corrosion J.*, 20 (2), (1985) 71-83.
24. Niles, W.D. and Sanders, H.R., "Reaction of Magnesium with Inorganic Constituents of Heavy Fuel Oil and Characteristics of Compounds Formed", *Trans. ASME, Ser.A*, 45 ( 1974) 611-619.
25. Fellows, J. A. "Metals Handbook, "Fractograph and Atlas of Fractographs", ASM Handbook Committee, 8<sup>th</sup> Edition, 1974, Vol.9.
26. Gouda, V. K. , Nassallah, M.M., Sayd, S.M. and Gerges, N.H., "Failure of Boiler Tubes in Power Plants", *Br. Corrosion. J.*, 16 (1981) No.1.
27. Francie, W., "Fuel Technology, a Summarised Manual", Pergamon Press, 1965.
28. Reed, R. D., " Furnace Operation", 3<sup>rd</sup> Edition, Gulf Publishing Company, 1981.
29. Rocca, E. Aranda, L., Moliere, M. and Steinmetz, P., "Nickel oxide as a new inhibitor of vanadium-induced hot corrosion of superalloys - comparison to MgO-based inhibitor", *J. Mater. Chem.*, 12 (2000) 3766-3772.
30. Smoth, H.J. and Harris, J.W., "Worked Examples in Engineering Thermody-namic", 2<sup>nd</sup> edn., MacDonal and Co.ltd., 1963.
31. Spiers, H.M. (Ed)., "Technical Data on Fuel", 6th Edition, London British World Power, 1998.
32. Mehl, R. F., "Metals Handbook, " Atlas of Microstructioure of Industrial Alloys," ASM Handbook committee, 8<sup>th</sup> Edn. Vol.7, 1971.

(2012) [www.jmaterenvironsci.com](http://www.jmaterenvironsci.com)